TABLE 3. CT Findings in Patients With PML

Disease	HL	Med-DLBCL	T-LBL
No. of patients	29 (44)	21 (32)	16 (24)
Tumor margins			
Well-defined margins	19 (66)	10 (48)	10 (62)
Ill-defined margins	10 (34)	11 (52)	6 (38)
Size of main mass (mean ± SD) (cm)	9.7 ± 2.8	9.7 ± 2.5	10.2 ± 3.3
Presence of surface lobulation*	20 (69)	7 (33)	4 (25)
Presence of vasular encasement†	2 (7)	13 (62)	6 (38)
Presence of chest wall invasion	4 (14)	4 (19)	2 (13)
Presence of cutaneous involvement	0	2 (10)	1 (6)
Presence of lung invasion	8 (28)	2 (10)	1 (6)
Presence of nodal involvement			
Cervical lymph node (superficial)*	3 (10)	0	7 (44)
Cervical lymph node (deep)†	9 (31)	0	9 (56)
Submandibular lymph node	0	0	1 (6)
Submental lymph node‡	0	0	2 (13)
Parotid lymph node‡	0	0	2 (13)
Supraclavicular lymph node§	3 (10)	0	8 (50)
Mediastinal lymph node†	28 (97)	14 (67)	8 (50)
Hilar lymph node‡	10 (34)	1 (5)	1 (6)
Axillary lymph node†	4 (14)	0	8 (50)
Celiac lymph node	3 (10)	0	1 (6)
Paraaortic lymph node*	6 (21)	0	6 (38)
Mesenteric lymph node‡	0	0	2 (13)
Iliac lymph node	0	0	1 (6)
Inguinal lymph node†	0	0	5 (31)
Presence of pleural effusion‡	6 (21)	12 (57)	8 (50)
Presence of pericardial effusion‡	5 (17)	10 (48)	9 (56)
Hepatomegaly‡	0	0	2 (13)
Splenomegaly†	1 (3)	1 (5)	11 (63)

Date in parentheses are percentages.
*$P < 0.01$, †$P < 0.001$, ‡$P < 0.05$, §$P < 0.0001$.
HL, Hodgkin lymphoma; Med-DLBCL, mediastinal diffuse large B-cell lymphoma; T-LBL, T-cell lymphoblastic lymphoma.

$P < 0.05$) was greater than that in HL (7% [2 of 29 patients], Figs. 1 and 2). Complete obstruction of the superior vena cava (SVC syndrome) was present in one of 29 patients with HL (3%), 4 of 21 with Med-DLBCL (19%), and 2 of 16 patients with T-LBL (13%). Forty-one of 66 tumors (62%) showed heterogeneous enhancement on CT, with no significant difference between 3 histologic subtypes.

Enlarged mediastinal nodes distinct from the primary lesion were present more commonly in HL (97% [28 of 29 patients]) than in Med-DLBCL (67% [14 of 21 patients], $P < 0.05$) and T-LBL (50% [8 of 16 patients], $P < 0.0001$, Table 3). Involvement of hilar nodes (Fig. 3) was significantly more common in HL (34% [10 of 29 patients]) compared with Med-DLBCL (5% [1 of 21 patients], $P < 0.05$) and T-LBL (6% [1 of 16 patients], $P < 0.05$). Involvement of bilateral axillary nodes was significantly more common in T-LBL (50% [8 of 16 patients]) than in Med-DLBCL (no patients, $P < 0.0001$) and HL (14% [4 of 29 patients], $P < 0.05$). Pleural effusion (Figs. 1 and 2) was significantly more common in Med-DLBCL (57% [12 of 21 patients], $P < 0.01$) or T-LBL (50% [8 of 16 patients], $P < 0.05$) than in HL (21% [6 of 29 patients]). Of the patients with pleural effusion, tumor cells were confirmed by cytology in 6 of 6 patients with HL (100%), in 5 of 12 with Med-DLBCL (42%), and in 2 of 8 patients (25%) with T-LBL. Pericardial effusion (Fig. 4) was significantly more common in T-LBL (56% [9 of 16 patients], $P < 0.01$) and Med-DLBCL (48% [10 of 21 patients], $P < 0.05$) than in HL (17% [5 of 29 patients]).

Statistically significant CT findings in the abdomen included splenomegaly, and involvement of paraaortic, mesenteric, and inguinal lymph nodes (Table 3). Splenomegaly was present more commonly in T-LBL (63% [11 of 16 patients]) than in HL (3% [1 of 29 patients], $P < 0.0001$) and Med-DLBCL (5% [1 of 21 patients], $P < 0.0001$). Involvement of abdominal paraaortic nodes (Fig. 1) was more common in T-LBL (38% [6 of 16 patients], $P < 0.01$) or HL (21% [6 of 29 patients], $P < 0.05$) than in Med-DLBCL (no patients). Involvement of inguinal (31% [5 of 16 patients]) or mesenteric lymph nodes (13% [2 of 16 patients]) was found only in T-LBL (Fig. 1). Extranodal lesions in the abdomen were proved pathologically in 3 patients. Two patients with Med-DLBCL had mass lesions in the stomach and kidney, and the

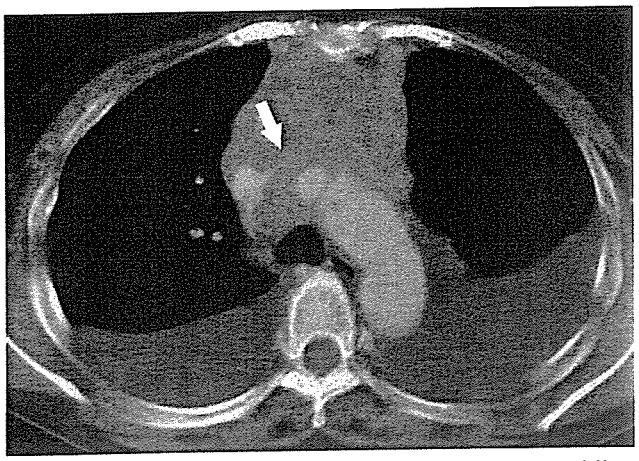

FIGURE 2. Thirty-two-year-old man with mediastinal diffuse large B-cell lymphoma (Med-DLBCL). CT image at the level of the aortic arch demonstrates a large, homogeneous enhancing anterior mediastinal mass without surface lobulation that compresses the left brachiocephalic vein (arrow). Also noted are bilateral pleural effusions.

other patient with HL had focal splenic mass. None of patients with T-LBL had evidence of extranodal involvement on the abdominal CT images.

There was excellent interobserver agreement for CT findings, including morphology and extent of main mass, enhancement pattern, lymph node enlargement, the presence of pleural effusion, pericardial effusion, hepatomegaly, and splenomegaly (Kappa = 0.82–1.00). Multiple logistic regression analysis demonstrated that the CT finding independently associated with increased likelihood of HL was surface lobulation ($P < 0.01$; Table 4), the absence of vascular involvement ($P < 0.01$), or pleural effusion ($P < 0.05$). The presence of vascular involvement was independently associated with increased likelihood of Med-DLBCL ($P < 0.001$, Table 4). In addition, CT findings including the presence of cervical lymph nodes or inguinal lymph nodes ($P < 0.001$; Table 4), the presence of pericardial effusion ($P < 0.05$), and the absence of surface lobulation ($P < 0.05$) were significantly associated with the likelihood of T-LBL.

DISCUSSION

Several studies have described the CT manifestations of PML. The typical presentation consists of an anterior mediastinal mass often associated with enlarged nodes in the middle and posterior mediastinum, and hila.[13–24] The mediastinal mass may involve vascular structures, pericardium, heart, pleura, lung, and chest wall on CT.[13–27] PML often affects extrathoracic sites at the time of diagnosis, particularly abdomen, head, and neck.[28,29]

The current study demonstrates that the different subtypes of PML often have characteristic manifestations that allow their distinction on CT. HL is characterized by the presence of a discrete anterior superior mediastinal mass with surface lobulation. Surface lobulation was present in 69% of patients with HL compared with 33% of patients with

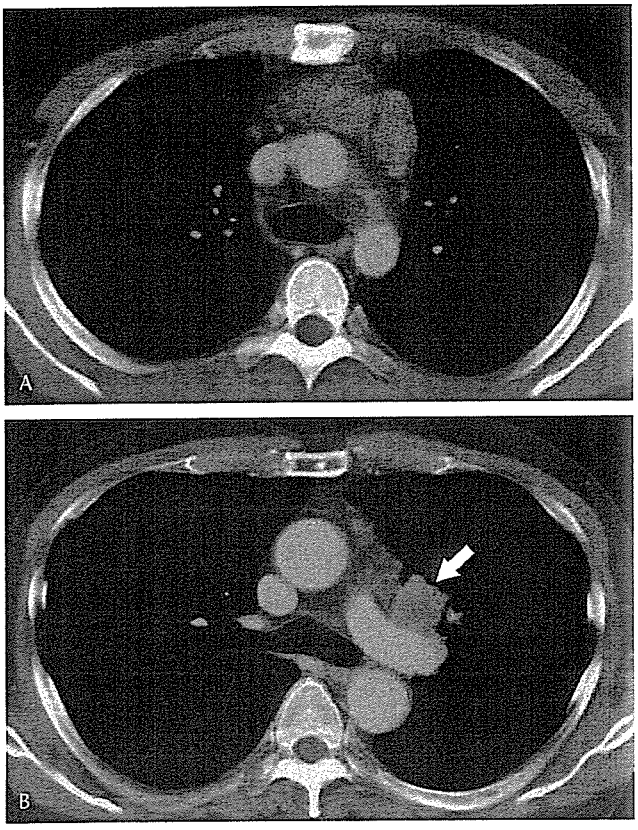

FIGURE 3. Twenty-nine-year-old man with Hodgkin's lymphoma (HL). A, Image at the level of the aortopulmonary window shows anterior mediastinal mass with surface lobulation and heterogeneous enhancement. B, Section obtained at the level of the carina demonstrates enlarged left hilar nodes (arrow).

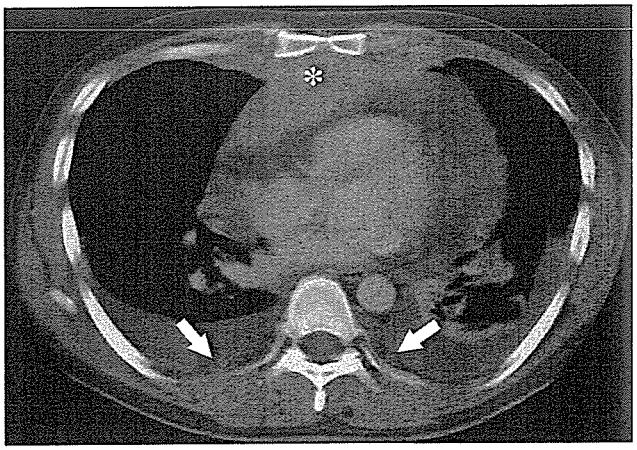

FIGURE 4. Thirty-two-year-old man with T-LBL. Image obtained at the level of the right ventricle shows a large anterior mediastinal mass (asterisk) with marked pericardial effusion. Also noted are pleural effusion bilaterally and soft-tissue nodular dissemination (arrows) in the pleura.

TABLE 4. Relationship Between CT Findings and the Likelihood of the PML Hisologic Subtypes

	CT findings	OR	95% CI	*P*
HL	Presence of surface lobulation	11.9	2.5–56.0	<0.01
	Absence of vascular involvement	11.8	1.9–71.9	<0.01
	Absence of pleural effusion	6.6	1.3–33.2	<0.05
Med-DLBCL	Presence of vascular involvement	7.5	2.3–24.1	<0.001
T-LBL	Presence of cervical or inguinal lymph node	33.9	4.7–244.6	<0.001
	Presence of pericardial effusion	11.4	1.7–77.6	<0.05
	Absence of surface lobulation	7.0	1.2–43.1	<0.05

HL, Hodgkin lymphoma; Med-DLBCL, mediastinal diffuse large B-cell lymphoma; T-LBL, T-cell lymphoblastic lymphoma; OR, odds ratio; CI, confidence interval.

Med-DLBCL and 25% with T-LBL. The surface lobulation of the main mass is due to involvement of multiple nodes and coalescence, a finding previously noted in HL at CT.[13,14] Enlarged nodes elsewhere in the mediastinum were seen in 97% of patients with HL in the current study and less commonly in the other subtypes.

Masses typically exhibit homogeneous soft-tissue attenuation, while large tumors may demonstrate heterogeneity with complex low attenuation representing necrosis, hemorrhage, and cystic degeneration.[20] Sixty-two percent of our cases showed heterogeneous enhancement on CT, with no significant difference between 3 histologic subtypes.

Med-DLBCL typically is initially confined to the mediastinum and contiguous nodal areas without showing extrathoracic disease at presentation.[3,5] Med-DLBCL may present with hematogenous spread to parenchymal organs such as kidney, liver, ovary, adrenal gland, gastrointestinal tract, and central nervous system during disease progression or at recurrence.[3] Extranodal involvement was found on the initial CT assessment and was confirmed by biopsy in 2 of our Med-DLBCL cases, whereas extrathoracic nodal involvement was not found in any of our patients with Med-DLBCL. Some observers consider that Med-DLBCL is a pathologic and clinical entity of non-Hodgkin lymphoma derived from mature thymic B-cells recognized by previous immunophenotypic studies.[30,31] However, the histogenesis is controversial, because Med-DLBCL can result in diffuse nodal involvement in advanced stages.[3,5]

Extrathoracic lymphadenopathy including superficial cervical, supraclavicular, submandibular, submental, parotid, mesenteric, and inguinal nodes, was seen in the majority of patients with T-cell lymphoblastic lymphoma in the present study. Another common finding in T-cell lymphoblastic lymphoma in the current study was the presence of splenomegaly, which was seen in 63% of cases. HL often involved axial lymph nodes including cervical, mediastinal, axillary, and paraaortic regions. However, none of the patients with HL in the current study had submandibular, submental, parotid, mesenteric, and inguinal lymphadenopathy. The low prevalence of nonaxial lymphadenopathy in HL had been recognized in previous studies.[29,32]

Diagnosis of subtypes in all patients was established by core or excisional biopsy in all cases. The ability to classify PML in small samples has improved considerably in the last few years because of progress of pathologic criteria and immunocytochemistry.[33,34] HL is characterized by a large inflammatory cell reaction within a fibrotic stroma, and the diagnosis is established by the identification of Hodgkin and Reed-Sternberg (HRS) cells.[2] Med-DLBCL is composed mainly of large clear cells within a characteristic background of compartmentalized fibrosis.[5] T-LBL is composed of a homogeneous population of immature lymphoblastic cells cytologically similar to acute lymphoblastic leukemia.[8–10] Biopsy provides sufficient information for the diagnosis of and subsequent therapeutic decision to treat patients with PML, because the definitive selection of therapeutic regimen is needed.

Our study has several limitations. It is retrospective and includes a relatively small number of patients. In clinical practice, the differential diagnosis would need to include a variety of other conditions that can present with an anterior mediastinal mass. However, we believe that the study demonstrates that the various histologic subtypes of PML have features on CT that allow distinction in the majority of cases. The anatomic distribution of the disease varies among the histologic subtypes of HL. Mediastinal involvement is most frequently seen in the nodular sclerosis HL subtype, while splenic involvement is more common in the mixed cellularity HL subtype.[29]

In conclusion, we found that CT findings often allowed differentiation of the various subtypes of PML. HL commonly presents as a mediastinal mass with surface lobulation and involves cervical, mediastinal, hilar, and paraortic nodes. Med-DLBCL demonstrates mediastinal mass without surface lobulation, often associated with vascular involvement, and pleural or pericardial effusion. T-LBL is characterized by mass without surface lobulation involving vascular structures often associated with pleural or pericardial effusion, by systemic nodal involvement including cervical, axillary, paraaortic, mesenteric, and inguinal, and by hepatomegaly and splenomegaly.

REFERENCES

1. Macchiarini P, Ostertag H. Uncommon primary mediastinal tumours. *Lancet Oncol.* 2004;5:107–118.
2. Keller AR, Castleman B. Hodgkin's disease of the thymus gland. *Cancer.* 1974;33:1615–1623.
3. Lazzarino M, Orlandi E, Paulli M, et al. Primary mediastinal B-cell lymphoma with sclerosis: an aggressive tumor with distinctive clinical and pathological features. *J Clin Oncol.* 1993;11:2306–2313.

4. Lichtenstein AK, Levine A, Taylor CR, et al. Primary mediastinal lymphoma in adults. *Am J Med.* 1980;68:509–514.
5. Perrone T, Frizzera G, Rosai J. Mediastinal diffuse large-cell lymphoma with sclerosis. A clinicopathologic study of 60 cases. *Am J Surg Pathol.* 1986;10:176–191.
6. Kirn D, Mauch P, Shaffer K, et al. Large-cell and immunoblastic lymphoma of the mediastinum: prognostic features and treatment outcome in 57 patients. *J Clin Oncol.* 1993;11:1336–1343.
7. Harris NL, Jaffe ES, Stein H, et al. A revised European-American classification of lymphoid neoplasms: a proposal from the International Lymphoma Study Group. *Blood.* 1994;84:1361–1392.
8. Nathwani BN, Kim H, Rappaport H. Malignant lymphoma, lymphoblastic. *Cancer.* 1976;38:964–983.
9. Cossman J, Chused TM, Fisher RI, et al. Diversity of immunological phenotypes of lymphoblastic lymphoma. *Cancer Res.* 1983;43:4486–4490.
10. Weiss LM, Bindl JM, Picozzi VJ, et al. Lymphoblastic lymphoma: an immunophenotype study of 26 cases with comparison to T cell acute lymphoblastic leukemia. *Blood.* 1986;67:474–478.
11. Onishi Y, Matsuno Y, Tateishi U, et al. Two entities of precursor T-cell lymphoblastic leukemia/lymphoma based on radiologic and immunophenotypic findings. *Int J Hematol.* 2004;80:43–51.
12. van Spronsen DJ, Vrints LW, Hofstra G, et al. Disappearance of prognostic significance of histopathological grading of nodular sclerosing Hodgkin's disease for unselected patients. *Br J Haematol.* 1997;96:322–327.
13. Heron CW, Husband JE, Williams MP. Hodgkin disease: CT of the thymus. *Radiology.* 1988;167:647–651.
14. Wernecke K, Vassallo P, Rutsch F, et al. Thymic involvement in Hodgkin disease: CT and sonographic findings. *Radiology.* 1991;181:375–383.
15. Luker GD, Siegel MJ. Mediastinal Hodgkin disease in children: response to therapy. *Radiology.* 1993;189:737–740.
16. North LB, Fuller LM, Hagemeister FB, et al. Importance of initial mediastinal adenopathy in Hodgkin disease. *AJR Am J Roentgenol.* 1982;138:229–235.
17. Bradley AJ, Carrington BM, Lawrance JA, et al. Assessment and significance of mediastinal bulk in Hodgkin's disease: comparison between computed tomography and chest radiography. *J Clin Oncol.* 1999;17:2493–2498.
18. Ha CS, Choe JG, Kong JS, et al. Agreement rates among single photon emission computed tomography using gallium-67, computed axial tomography and lymphangiography for Hodgkin disease and correlation of image findings with clinical outcome. *Cancer.* 2000 15;89:1371–1379.
19. Diederich S, Link TM, Zuhlsdorf H, et al. Pulmonary manifestations of Hodgkin's disease: radiographic and CT findings. *Eur Radiol.* 2001;11:2295–2305.
20. Shaffer K, Smith D, Kirn D, et al. Primary mediastinal large-B-cell lymphoma: radiologic findings at presentation. *AJR Am J Roentgenol.* 1996;167:425–430.
21. Strollo DC, Rosado-de-Christenson ML, Jett JR. Primary mediastinal tumors: Part II. Tumors of the middle and posterior mediastinum. *Chest.* 1997;112:1344–1357.
22. Spiers AS, Husband JE, MacVicar AD. Treated thymic lymphoma: comparison of MR imaging with CT. *Radiology.* 1997;203:369–376.
23. Schwartz EE, Conroy JF, Bonner H. Mediastinal involvement in adults with lymphoblastic lymphoma. *Acta Radiol.* 1987;28:403–407.
24. Chaignaud BE, Bonsack TA, Kozakewich HP, et al. Pleural effusions in lymphoblastic lymphoma: a diagnostic alternative. *J Pediatr Surg.* 1998;33:1355–1357.
25. Press GA, Glazer HS, Wasserman TH, et al. Thoracic wall involvement by Hodgkin disease and non-Hodgkin lymphoma: CT evaluation. *Radiology.* 1985;157:195–198.
26. Cho CS, Blank N, Castellino RA. Computerized tomography evaluation of chest wall involvement in lymphoma. *Cancer.* 1985;55:1892–1894.
27. Bonomo L, Ciccotosto C, Guidotti A, et al. Staging of thoracic lymphoma by radiological imaging. *Eur Radiol.* 1997;7:1179–1189.
28. The International Non-Hodgkin's Lymphoma Prognostic Factors Project. A predictive model for aggressive non-Hodgkin's lymphoma. *N Engl J Med.* 1993;329:987–994.
29. Jaffe ES, Harris NL, Stein H, et al, eds. World Health Organization Classification of tumours. Pathology and genetics of tumours of haematopoietic and lymphoid tissues. Lyon, France: IARC Press, 2001.
30. Addis BJ, Isaacson PG. Large cell lymphoma of the mediastinum: a B cell tumour of probable thymic origin. *Histopathology.* 1986;10:379–390.
31. Davis RE, Dorfman RF, Warnke RA. Primary large-cell lymphoma of the thymus: a diffuse B-cell neoplasm presenting as primary mediastinal lymphoma. *Hum Pathol.* 1990;21:1261–1268.
32. Hoelzer D, Gokbuget N, Digel W, et al. Outcome of adult patients with T-lymphoblastic lymphoma treated according to protocols for acute lymphoblastic leukemia. *Blood.* 2002;99:4379–4385.
33. Ben-Yahuda D, Polliack E, Okon Y, et al. Image-guided core-needle biopsy in malignant lymphoma: experience with 100 patients that suggests the techniques reliable. *J Clin Oncol.* 1996;14:2431–2424.
34. Van Besien K, Kelta M, Bahaguna P. Primary mediastinal B-cell lymphoma: a review of pathology and management. *J Clin Oncol.* 2001;15:1855–1864.

Original Paper

Hepatic Arterial Infusion of 5-Fluorouracil and Extrabeam Radiotherapy for Liver Metastases from Pancreatic Carcinoma

Hiroshi Ishii, Junji Furuse, Michitaka Nagase, Masahiro Yoshino
Mitsuhiko Kawashima[1], Mitsuo Satake[1], Takashi Ogino[1], Hiroshi Ikeda[1]
Division of Hepatobiliary Pancreatic Medical Oncology and [1]Department of Radiology
National Cancer Center Hospital East, Kashiwa, Japan
Corresponding Author: Hiroshi Ishii MD, National Cancer Center Hospital East, 6-5-1 Kashiwanoha, Kashiwa, Chiba 277-8577, Japan
Tel: +81 471 33 1111, Fax: +81 471 31 4724, E-mail: hirishii@east.ncc.go.jp

ABSTRACT

Background/Aims: To examine the efficacy and safety of a combined modality therapy consisting of hepatic arterial infusion of 5-fluorouracil and external-beam radiotherapy in patients with advanced pancreatic carcinoma.

Methodology: Hepatic arterial infusion chemotherapy consisted of 5-FU 1000mg/m^2 administrated as a 5-hr continuous infusion once weekly. External-beam radiotherapy (total dose, 50Gy; 2Gy/day) was delivered to the pancreas tumor concurrently for 5-6 weeks. Seventeen patients with no distant metastases except to the liver were enrolled in this study.

Results: Patients received a median of 13 cycles of chemotherapy. Sixteen of 17 patients received a total radiotherapy dose of 50Gy. In one patient, treatment was discontinued after 24Gy of radiotherapy and 2 cycles of chemotherapy because of progressive disease. Nausea and vomiting were the most common types of toxicity. Grade 3 or worse toxicity was observed in 2 patients. Four patients developed gastroduodenal ulcers. Of the 16 patients, 7 (41%) showed a partial response, and 9 (53%) showed no change. The median overall survival was 4.5 months and 1-yr overall survival of 11.8% was observed.

Conclusions: The combined therapy is active and well tolerated, but results in a poorer prognosis, in spite of its high initial response rate.

KEY WORDS: Pancreatic carcinoma; Liver metastasis; Hepatic arterial infusion; 5-fluorouracil; Radiotherapy

ABBREVIATIONS: Hepatic Arterial Infusion (HAI); External-Beam Radiotherapy (EBRT); 5-fluorouracil (5-FU); Partial Response (PR); No Change (NC); Progressive Disease (PD); Carbohydrate Antigen 19-9 (CA19-9); Computed Tomography (CT); World Health Organization (WHO)

INTRODUCTION

Liver metastasis is a common progression of pancreatic carcinoma and the prognosis of patients in whom it occurs is extremely poor. Although gemcitabine has been shown to be an active agent in the treatment of advanced pancreatic carcinoma, it has not been observed to adequately prolong patient survival (1). Hepatic arterial infusion (HAI) of 5-fluorouracil (5-FU) has been performed in several clinical trials in patients with liver metastasis from colorectal cancer and the findings indicate that HAI results in a high response rate (2,3). In addition, with regard to pancreatic carcinoma, recent study of HAI chemotherapy after vascular supply distribution via superselective embolization has also demonstrated promising results (4). At the present time, combined external-beam radiation therapy (EBRT) and 5-FU therapy are considered standard treatment for locally advanced pancreatic carcinoma (5-7). Thus, EBRT combined with HAI therapy using 5-FU is thought to have high clinical applicability and may prove beneficial to patients with pancreatic carcinoma without distant metastases, except to the liver. We therefore conducted a phase 2 study of combined EBRT and HAI using 5-FU to clarify the efficacy and safety of this treatment in patients with pancreatic carcinoma with metastasis restricted to the liver.

METHODOLOGY

Seventeen patients with advanced pancreatic cancer complicated by liver metastasis underwent HAI chemotherapy and EBRT between February 1998 and November 2000 at the National Cancer Center Hospital East. The eligibility criteria for inclusion in this study were: 1) histological proof of adenocarcinoma of the pancreas, 2) no distant metastases on computed tomography (CT) staging, except to the liver, 3) no previous anti-cancer treatment, 4) a performance status of 0, 1, or 2 according to the World Health Organization (WHO) grading system (8), 5) adequate bone marrow functioning (blood cell count of 4,000 or greater, platelet count of 100,000 or greater, and hemoglobin of 10g/dL or greater), adequate renal function (serum creatinine level of less than 1.1mg/dL), and adequate hepatic function (serum bilirubin level of less than 3.0mg/dL, serum alanine and aspartate transaminase levels of less than 200 IU/L), 6) no serious complications, and 7) receipt of written informed consent from the patient. Percutaneous biliary drainage was performed in patients with obstructive jaundice, and patients were required to have a total serum bilirubin level of less than 3.0mg/dL before initiation of treatment. Patient characteristics are summarized in **Table 1**.

Hepatic arteriography was performed prior to

Hepato-Gastroenterology 2004; 51:1175-1178

TABLE 1 Patient Characteristics

Characteristic	No. of patients (%)
Gender	
Male	11 (65%)
Female	6 (35%)
Median age (range)	59 (50-77)
WHO performance status	
0	5 (29%)
1	10 (59%)
2	2 (12%)
Location of primary tumor	
Head	5 (29%)
Body/tail	12 (71%)
Median CEA, ng/mL (range)	8.6 (0.8-185)
Median CA 19-9, U/mL (range)	827 (21-14552)

WHO: World Health Organization;
CEA: carcinoembryonic antigen;
CA 19-9: carbohydrate antigen 19-9.

catheter placement to determine the degree of arterial blood supply to the liver. The gastroduodenal and right gastric arteries of all patients were ligated with steel coils to prevent drug perfusion into the stomach and the duodenum. A catheter was positioned in the gastroduodenal artery. Catheters were placed via the left subclavian artery. The port was connected to the catheter and implanted in the subcutaneous space of the left chest wall.

After implanting the catheter and the port, 5-FU (1,000mg/m^2) mixed with 100mg of hydrocortisone (Solu-Cortef; Pharmacia & Upjohn, New Jersey, USA) and 5,000 U of heparin, was administrated over 5 hours through a battery-operated ambulatory infusion pump. After drug infusion, 20mL of saline and 5,000 U of heparin were infused through the pump. Cycles of intra-arterial infusion were repeated once weekly, unless there was evidence of disease progression or unacceptable toxicity levels.

Radiation therapy was delivered using the conformal, arc rotation technique to deliver a 10-MV X-ray, in order to achieve a total dose of 50Gy, given in 25 fractions over 5 weeks. The radiation field included the primary tumor and a 1- to 3-cm margin which covered the pancreaticoduodenal and celiac axis lymph nodes. This field was defined during treatment-planning CT one or two days before radiation therapy.

The toxicity of treatment was scored weekly according to WHO criteria (8). Both radiotherapy and chemotherapy were suspended if grade 3 toxicity was encountered, and resumed upon recovery to a grade 2 level of toxicity.

Follow-up CT was performed every month for 6 months, and every 2 months thereafter, in order to assess objective tumor responses according to WHO criteria. Local progression was diagnosed when the primary tumor was enlarged on CT, or when obstructive jaundice occurred after treatment. Overall survival was measured from the first day of treatment, and the survival rate was calculated by the Kaplan-Meier method (9). Serum CA 19-9 levels were measured every month by immunoradiometric assay using the Centocor radioimmunoassay kit (Centocor, Inc., Malvern, PA).

Patients received a full explanation about this study and gave written informed consent after approval of the protocols by the Institutional Review Board of the National Cancer Center.

RESULTS

A total of 251+ cycles of HAI chemotherapy were administrated (median 13, range 2-34+). Of 17 patients, 16 received EBRT with a total dose of 50Gy. In the remaining patient, treatment was discontinued after receipt of 24Gy of EBRT and 2 cycles of HAI because of disease progression. Therapy was discontinued due to disease progression in 14 patients, hepatic arterial obstruction in 1, and duodenal ulcer in 1. One patient was still receiving HAI chemotherapy at the time of writing.

Manifestations of treatment-related toxicity are summarized in **Table 2**. No life-threatening toxicity was observed, but 2 patients (12%) encountered Grade 3 toxicity. Nausea and vomiting were the most common types of toxicity. Four patients developed gastroduodenal ulcers after EBRT. Of these patients, one required hospitalization due to bleeding, and another

TABLE 2 Treatment-Related Toxicity according to WHO Criteria

	No. of patients (%)	
	Grade	
Toxicity	2	3
Leucopenia	3 (18%)	0
Anemia	0	0
Thrombocytopenia	3 (18%)	0
Nausea/vomiting	6 (35%)	2 (12%)
Liver dysfunction	0	0
Diarrhea	0	0
Mucositis	0	0

WHO: World Health Organization.

TABLE 3 Changes in the CA 19-9 levels of Patients with Elevated CA 19-9 Levels after Treatment (>100 U/mL)

	CA 19-9 (U/mL)		Tumor	Survival
Case no.	Before *	After #	response$	(days)
1	14552		NC	80
2	13216		PD	35
3	9945		PR	84
4	3944	673	PR	402
5	3091	292	NC	86
6	1739	53	PR	349
7	1526		NC	136
8	1428		NC	133
9	827		NC	114
10	318		PR	264
11	212		NC	114
12	170	41	NC	234

CA 19-9: carbohydrate antigen 19-9, NC: no change, PR: partial response, PD: progressive disease. *Maximal levels before treatment are represented; #Minimal levels after treatment are represented where responses were observed; $Assessed by computed tomography.

TABLE 4 Patterns of Initial Disease Progression

	No. of patients
Peritoneum (ascites)	6
Peritoneum and lymph node	1
Liver	2
Liver and lymph node	1
Liver and bone	1
Lymph node	1
Bone	1

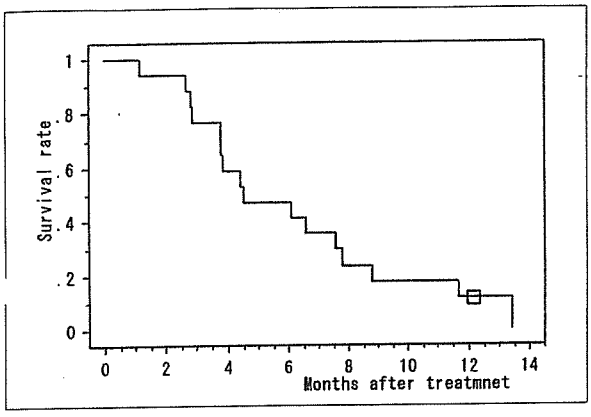

FIGURE 1 Overall survival curve for 17 patients treated with radiation and hepatic arterial 5-fluorouracil infusion. An open square indicates a censored case.

discontinued HAI therapy because of a refractory duodenal ulcer 5 months after initiation of treatment.

Seven (41%) patients had partial responses, 9 (53%) remained stable, and one showed progressive disease. Serum CA 19-9 levels were reduced by more than 50% in 4 of 12 patients (33%) who had pretreatment CA 19-9 levels of 100 U/mL or greater **(Table 3)**. Death from cancer was documented in 16 patients at the time of analysis. The initial sites of disease progression were documented in 13 patients **(Table 4)**. Peritoneal dissemination was the main cause of progression. Overall survival curves are shown in **Figure 1**. The median overall survival was 4.5 months and 1-yr overall survival was 11.8% observed.

DISCUSSION

Systemic chemotherapy using gemcitabine is considered standard therapy for advanced pancreatic carcinoma. However, a tumor response rate of only 5.4% and a survival time of 5.65 months have been observed with gemcitabine treatment, neither of which are satisfactory outcomes (1). High response rates of liver metastasis to HAI in patients with colorectal carcinoma have been reported (2,3,10). In a previous study (10), we employed continuous HAI of 5-FU for 5 days at a dose of 500mg/m^2/day every 4 weeks in order to treat liver metastasis from pancreatic carcinoma. The treatment was feasible but the overall response rate was only 8% at this dose and schedule. For treatment of liver metastasis from colorectal carcinoma, Arai *et al.* (3) reported a response rate of 78% after intermittent HAI of high-dose 5-FU once a week on an outpatient basis. In accordance with phase 1 and 2 studies, we therefore tried weekly HAI of 5-FU at a dose of 1000mg/m^2 for treatment of isolated liver metastasis from pancreatic carcinoma.

The toxicity associated with this regimen seemed to be mild. In the current study, grade 4 toxicity was not observed and the percentage of patients with grade 3 or worse toxicity was low (12%). Throughout the course of treatment, hematological toxicity was frequent but mild, and gastrointestinal toxicity was the only cause of treatment interruption. In a previous pilot study (11), hepatic artery occlusion was observed in 23% of patients and was the second cause of treatment discontinuation. However, occlusion of the hepatic artery occurred in only one patient (6%) in the current study. The frequency of hepatic artery thrombosis due to 5-FU infusion seemed to be lower with use of the intermittent schedule. On the other hand, gastroduodenal ulcers were frequently observed (24%), compared to a previous study in which HAI was administered continuously (8%) (11).

In the current study, an objective tumor response of 41% was noted following CT assessment. Serum CA 19-9 levels were reduced in 33% of patients with high initial CA 19-9 levels. Nine of the patients (53%) responded to therapy, as evaluated by CT or measurement of CA 19-9 levels. Greater response rates were observed with combination therapy than with any other form of systemic chemotherapy in the treatment of advanced pancreatic carcinoma. However, high response rates did not translate into prolonged survival for the patients in this study. For example, one of the patients who responded to treatment died due to peritoneal dissemination only 2.8 months after the initiation of the treatment. As shown in **Table 4**, peritoneal dissemination was the major cause of treatment failure. Hepatic extraction of 5-FU after HAI was estimated to be between 15-50% (12), thus, we expected a 150-500mg/m^2 weekly dose of 5-FU to produce a systemic anti-tumor effect. However, this dose seemed insufficient to reduce distant metastases, especially peritoneal dissemination. Surgical exploration revealed minute peritoneal metastasis in 12.5% of patients who had no distant metastases but locally unresectable pancreatic carcinoma, as assessed by CT staging (13).

Recently, excellent results have been reported using arterial infusion chemotherapy at the primary site of pancreatic carcinoma (4,14). In these reports, regional chemotherapy for pancreatic carcinoma was repeated for as long as catheters remained patent without occlusion or dislocation. Long-term tumor control might be obtained via this method, provided the tumor is responsive to the agent being infused. With respect to radiotherapy, however, it would be difficult to deliver a dose exceeding 72Gy to the pancreatic region, regardless of whether or not the tumor is responsive to radiotherapy (15). We will not select a higher dose of EBRT in combination with HAI in our next trial because we do not believe intensification of radiotherapy can reduce distant progression in pancreatic cancer patients. We do not know whether regional chemotherapy has the ability to reduce peri-

toneal dissemination from pancreatic carcinoma. However, this might explain the prolonged survival of patients in studies involving regional chemotherapy (4,14).

We conclude that liver metastasis from pancreatic cancer responds well to HAI, but that combination therapy fails to prolong the survival of such patients. Thus, we do not feel that a radiotherapeutic approach can be used to treat patients with pancreatic carcinoma who do not have distant metastases, except to the liver, as evaluated by clinical staging. Therefore, HAI should be used in combination with either systemic chemotherapy or regional chemotherapy at the primary site.

REFERENCES

1 **Burris HA 3rd, Moore MJ, Andersen J, Green MR, Rothenberg ML, Modiano MR, Cripps MC, Portenoy RK, Storniolo AM, Tarassoff P, Nelson R, Dorr FA, Stephens CD, Von Hoff DD:** Improvements in survival and clinical benefit with gemcitabine as first-line therapy for patients with advanced pancreatic cancer: a randomized trial. J Clin Oncol 1997; 15:2403-2413.

2 **Sugihara K:** Continuous hepatic arterial infusion of 5-fluorouracil for unresectable colorectal liver metastases: phase 2 study. Surgery 1995; 117:624-628.

3 **Arai Y, Inaba Y, Takeuchi Y, Ariyoshi Y:** Intermittent hepatic arterial infusion of high-dose 5FU on a weekly schedule for liver metastases from colorectal cancer. Cancer Chemother Pharmacol 1997; 40:526-530.

4 **Homma H, Doi T, Mezawa S, Takada K, Kukitsu T, Oku T, Akiyama T, Kusakabe T, Miyanishi K, Niitsu Y:** A novel arterial infusion chemotherapy for the treatment of patients with advanced pancreatic carcinoma after vascular supply distribution via superselective embolization. Cancer 2000; 89:303-313.

5 **Moertel CG, Childs DS, Reitemeier RJ, Colby MY, Holbrook MA:** Combined 5-fluorourail and supervoltage radiation therapy of locally unresectable gastrointestinal cancer. Lancet 1969; 2:865-867.

6 **The Gastrointestinal Tumor Study Group:** Therapy of locally unresectable pancreatic carcinoma: a randomized comparison of high dose (6000 rads) radiation alone, moderate dose radiation (4000 rads + 5-fluorouracil), and high dose radiation + 5-fluorouracil. Cancer 1981; 48:1705-1710.

7 **Gastrointestinal Tumor Study Group:** Treatment of locally unresectable carcinoma of the pancreas: comparison of combined-modality therapy (chemotherapy plus radiotherapy) to chemotherapy alone. J Natl Cancer Inst 1988; 80:751-755.

8 **World Health Organization:** WHO Handbook for Reporting Results of Cancer Treatment. offset publication 48. Geneva, World Health Organization, 1979.

9 **Kaplan EL, Meier P:** Nonparametric estimation from incomplete observations. J Am Stat Assoc 1958; 63:457-481.

10 **Harmantas A, Rotstein L, Langer B:** Regional versus systemic chemotherapy in the treatment of colorectal carcinoma metastatic to the liver. Is there a survival difference? Meta-analysis of the published literature. Cancer 1996; 78:1639-1645.

11 **Furuse J, Maru Y, Yoshino M, Mera K, Sumi H, Tajiri H, Satake M, Onaya H, Ishikura S, Ogino T, Kawashima M, Ikeda H:** Hepatic arterial infusion of 5-fluorouracil for liver metastases from pancreatic carcinoma: results from a pilot study. Hepatogastroenterology 2001 48:208-211.

12 **Collins JM:** Pharmacologic rationale for regional drug delivery. J Clin Oncol 1984; 2:498-504.

13 **Furuse J, Ogino T, Ryu M, Kinoshita T, Konishi M, Kawano N, Ishikura S, Shimizu W, Sekiguchi R, Moriyama N, Iwasaki M, Yoshino M:** Intraoperative and conformal external beam radiation therapy in patients with locally advanced pancreatic carcinoma; results from a feasibility phase II study. Hepatogastroenterology 2000; 47:1142-1146.

14 **Ohigashi H, Ishikawa O, Imaoka S, Sasaki Y, Kabuto T, Kameyama M, Furukawa H, Hiratuka M, Nakamori S, Nakano H, Yasuda T, Iwanaga T:** A new method of intra-arterial regional chemotherapy with more selective drug delivery for locally advanced pancreatic cancer. Hepatogastroenterology 1996; 43:338-345.

15 **Ceha HM, van Tienhoven G, Gouma DJ, Veenhof CHN, Schneider CJ, Rauws EAJ, Phoa SSKS, Gonzalez DG:** Feasibility and efficacy of high dose conformal radiotherapy for patients with locally advanced pancreatic carcinoma. Cancer 2000; 89:2222-2229.

Synovial Sarcoma of the Soft Tissues

Prognostic Significance of Imaging Features

Ukihide Tateishi, MD, PhD, Tadashi Hasegawa, MD, PhD, Yasuo Beppu, MD, Mitsuo Satake, MD, and Noriyuki Moriyama, MD, PhD

Objective: This study assessed the prognostic value of computed tomography (CT) and magnetic resonance (MR) imaging features in synovial sarcoma of the soft tissues.

Methods: CT and MR imaging studies were performed in 30 patients with pathologically confirmed synovial sarcoma of the soft tissues. CT and MR imaging findings obtained by 2 radiologists with agreement by consensus were compared for histopathologic features including tumor grade. Univariate analyses were conducted to clarify the impact of imaging findings on overall survival with a medium duration of 32 months. Multivariate analysis was estimated using a Cox proportional hazards model with the relative risk of each variable.

Results: Statistically significant imaging findings favoring a diagnosis of high-grade tumor included proximal distribution ($P < 0.01$), large tumor size (>10 cm, $P < 0.05$), the absence of calcification ($P < 0.05$), tumor possessing cyst ($P < 0.01$), the presence of hemorrhage ($P < 0.05$), and the presence of triple signal pattern ($P < 0.05$). Univariate analysis showed that proximal distribution ($P < 0.05$), tumor size larger than 5 cm ($P < 0.01$), the absence of calcification ($P < 0.01$), the presence of hemorrhage ($P < 0.05$), and the presence of triple signal pattern ($P < 0.05$) had a significant association with the disease-free survival (DFS). Multiple logistic regression models revealed that tumor size larger than 10 cm had a significant impact on the DFS with relative risk of 18.8 ($P < 0.05$).

Conclusion: CT and MR imaging studies allow prognosis prediction in patients with synovial sarcoma of the soft tissues.

Key Words: computed tomography, magnetic resonance imaging, synovial sarcoma

(*J Comput Assist Tomogr* 2004;28:140–148)

From the Divisions of Diagnostic Radiology (Drs Tateishi, Satake, and Moriyama), Pathology (Dr Hasegawa), and Orthopedics (Dr Beppu), National Cancer Center Hospital and Research Institute, Tokyo, Japan.

This work was carried out by the Program for Promotion of Fundamental Studies in Health Sciences of the Organization for Pharmaceutical Safety and Research (Japan) and was supported in part by a Grant-in-Aid for Cancer Research from the Ministry of Health, Labor and Welfare.

Reprints: Ukihide Tateishi, MD, PhD, Division of Diagnostic Radiology, National Cancer Center Hospital, 5-1-1, Tsukiji, Chuo-Ku, Tokyo 104-0045, Japan (e-mail: utateish@ncc.go.jp).

Synovial sarcoma is the fourth most common soft tissue sarcoma, comprising 10% of all soft tissue sarcomas and arising most frequently in the extremities, generally in the vicinity of the joints, bursae, and tendon sheaths.[1–3] Synovial sarcoma is a morphologically high-grade sarcoma that has been extensively described.[4–6] However, some patients develop metastases quite early after surgery and die of disease whereas a distinct group of patients have prolonged courses without recurrence or metastasis. For these reasons, it is imperative that accurate tumor grading should be made to determine the prognoses for patients in synovial sarcoma of the soft tissues.

Several studies showed that the characteristic features in synovial sarcoma of the soft tissues are nonspecific and attributable mainly to heterogeneity which includes necrosis, calcification, and hemorrhage.[7–18] Tumors appear on T2-weighted MR images as soft tissue masses of marked heterogeneity often associated with various degrees of internal septa.[8–12] However, the relationships between these imaging features and the prognoses for patients were not fully understood. We undertook this retrospective study in a series of patients with synovial sarcoma of the soft tissues to assess the prognostic value of computed tomography (CT) and magnetic resonance (MR) imaging features.

PATIENTS AND METHODS

Patients

We reviewed the cases of 30 patients with synovial sarcoma of the soft tissues who were registered in our pathology files. The clinical details, including follow-up information, were obtained by reviewing all the medical charts. Eighteen (60%) of the 30 patients were female and 12 (40%) were male. Their median age at diagnosis was 27 years and ranged from 10 to 61 years. No patients were lost to follow-up, which began on the date of primary surgery. The median duration of follow-up was 32 months and ranged from 0 to 95 months. Disease-free survival (DFS) was recorded as the time from diagnosis to death due to any cause. Both metastasis-free survival (MFS) and recurrence-free survival (RFS) were also calculated.

An expert pathologist, who had developed the tumor grading system that we used, reviewed for diagnosis the histo-

logic slides of all the tumors of patients. Immunohistochemical staining was carried out in all patients to confirm the diagnosis or tumor type according to the classification system described by Enzinger and Weiss.[3] Histologically, 14 tumors (47%) were classified as monophasic fibrous subtype, 11 (37%) as biphasic, and 5 (17%) as poorly differentiated. In this study, the histological grade of each tumor was determined using a grading system established by Hasegawa et al.[19–21] According to this grading system, synovial sarcomas were assigned low- or high-grade: low-grade, n = 6 (20%); high-grade, n = 24 (80%). Excised specimens were available for review or for mapping correlation with images.

Imaging Studies

Images reviewed included CT scans (all with pre- and postcontrast enhancement) and MR images (in all patients with contrast enhancement). CT scanning was performed with 1 of 2 models in all patients (Aquilion V-detector CT scanner or X-Vigor helical CT scanner, Toshiba Medical Systems, Tokyo, Japan). On average, initial CT scans and MR examinations on all patients were performed within 10 days. Scanning parameters for CT scans were axial single or 4-slice mode, 4.0-mm section thickness, 0.5 or 1.0 seconds/rotation, 120–150 kVp, and 200–250 mA. Images were reconstructed at 10.0-mm slice thickness using a standard algorithm without edge enhancement. MR imaging was performed using 1 of 2 models of 1.5-T systems (General Electric Medical Systems, Milwaukee, WI, or Toshiba Medical Systems, Tokyo, Japan). T1-weighted spin-echo MR images (TR/TE: 400 to 750/8 to 17 milliseconds) were obtained in the transverse plane using a dedicated body or surface coil. Using the spin-echo or fast spin-echo technique, T2-weighted images (TR/TE_{eff}: 2000 to 7000/117 to 144 milliseconds; 12–16 echo train) were then obtained in transverse and coronal planes. The images were obtained with a field of view of 16–26 cm, an image matrix of 128 × 160 to 256, a slice thickness of 4–10 mm, 0.4–1.0 mm gap, and 1–4 signals acquired. Postcontrast fat-saturated T1-weighted images were obtained in transverse and coronal planes after the intravenous administration of 0.1 mmol/kg of gadopentetate dimeglumine (Magnevist; Nihon-Shering, Osaka, Japan).

Image Analysis

All CT and MR images were reviewed by 2 radiologists and the findings were reported as a consensus opinion. The lesions were judged according to the characteristics of imaging features that included tumor size, location, depth (superficial or deep), types of margin, calcification, internal septa, cystic component, hemorrhage, fluid-fluid level, triple signal pattern, signal characteristics on T1- and T2-weighted images, and homogeneity (homogeneous or heterogeneous). Superficial tumor (dermal or subcutaneous tumor) was exclusively located above the superficial fascia without invasion of the fascia. Deep tumor was located either exclusively beneath the superficial fascia or superficial to the fascia with invasion of or through the fascia. Tumors arising from the knee, ankle, foot, forearm, and hand were included in the distal lesions. Tumors arising from the neck, trunk, femur, and inguinal regions were contained in the proximal lesions.

The signal characteristics were mainly described as isointense or hyperintense relative to the signal intensity of skeletal muscle. Triple signal pattern—characterized by the presence of high signal similar to that of fluid, intermediate signal intensity equal to or slightly hyperintense relative to fat, and low signal intensity closer to that of fibrous tissue—was also noted. Enhancement of the lesion signal intensity was assessed after contrast material injection and was categorized as either none, weak, or marked compared with those of the surrounding skeletal muscles. Homogeneity of enhancement was categorized as homogeneous or heterogeneous and also recorded.

Statistical Analysis

The demographics and imaging characteristics of patients were compared using the Wilcoxon rank sum test for continuous variables and the χ^2 or Fisher exact test probability tests for categorized variables. Univariate analysis was performed by comparing Kaplan-Meier survival curves and carrying out log-rank tests. The relative risk of each variable subjected to multivariate analysis was estimated using a Cox proportional hazards model. All analyses were conducted using SPSS software (version 11.0J; SPSS, Chicago, IL). Differences and correlations at a P value of <0.05 was considered to be statistically significant.

RESULTS

The median age at the time of presentation was 27 years and 9 patients (30%) were under 20 years of age. The tumors were located on the extremities in 22 (73%) pateints, trunk in 7 (23%), and neck in 1 (4%). The median tumor size was 7 cm and ranged from 2.2 to 15.0 cm. Twenty-five (83%) tumors were situated deeply, and 5 (17%) were superficial. The surgical procedures performed consisted of wide excision, amputation, or disarticulation with adequate surgical margins in 17 (57%) patients and marginal or intralesional excision with marginal or inadequate margins in 14 (43%). Additional treatment included chemotherapy in 22 (73%) patients, radiotherapy in 1 (3%), and both in 5 (17%). Metastases occurred in 11 (37%) of the 30 patients, and the locations were the lung in 6 (20%) patients, soft tissue in 2 (7%), bone in 2 (7%), brain in 2 (7%), and abdominal dissemination in 2 (7%), respectively. Nine (30%) patients developed local recurrences.

On both CT and MR images, 16 (53%) and 14 (47%) of 30 tumors had regular and irregular tumor contours, respectively. Twenty-two (73%) tumors were attached or located adjacent to muscular tendons. Calcifications that appeared as

round, punctate (Fig. 1) and dense (Fig. 2) were identified on unenhanced CT images in 3 (10%) low-grade and 5 (17%) high-grade tumors, respectively. The lesion usually appeared as a heterogeneous soft tissue mass and may have a multilocular appearance with various degrees of internal septations. On T2-weighted MR images, tumors predominately showed increased signal intensity relative to that of the skeletal muscle (Fig. 3), and the images showed heterogeneous appearance with internal septa of low intensity. Internal septa were found in 20 (67%) tumors on T2-weighted MR images. Cystic components (Fig. 4) were seen in 19 (63%) patients with high-grade tumor. Of these, 4 (13%) cases showed multilocular cystic lesions within the tumor. High intensity signals on T1-weighted MR images highly suggestive of hemorrhage (Fig. 3) were found in 14 (47%) patients with high-grade tumors. Of these tumors associated with hemorrhage, 5 (17%) tumors contained fluid-fluid levels on T2-weighted MR images. Triple signal pattern (Fig. 5) was seen in 13 (43%) patients with high-grade tumor. All tumors showed marked enhancement compared with those of the adjacent skeletal muscles on contrast-enhanced MR images. Contrast-enhanced MR images revealed homogeneous and heterogeneous enhancement (Fig. 4) in 5 (17%) and 25 (83%) tumors, respectively.

The results of the statistical analysis are summarized in Tables 1 to 3. Statistically significant imaging findings favoring a diagnosis of high-grade tumor included proximal distribution ($P < 0.01$), large tumor size (>10 cm, $P < 0.05$), the absence of calcification ($P < 0.05$), tumor possessing cyst ($P < 0.01$), the presence of hemorrhage ($P < 0.05$), and the presence of triple signal pattern ($P < 0.05$). Imaging features including cyst, hemorrhage, triple signal pattern, and fluid-fluid levels were found only in high-grade tumors. At the last follow-up, 9 of the 30 (30%) patients had died of their disease and 21 (70%) were alive with or without metastatic disease, with 5-year DFS rates of 48%. Both MFS and RFS rates were 58% and 65%, respectively. There was a significant difference in 5-year DFS rates between low- and high-grade tumors (100% vs. 26%, $P < 0.05$). Significant difference was also found in the MFS between low- and high-grade tumors (100% vs. 14%, $P < 0.05$) whereas not in the RFS (100% vs. 47%, $P = 0.07$). The univariate analysis revealed that proximal distribution ($P < 0.05$; Fig. 6), tumor size larger than 5 cm ($P < 0.01$, Fig. 7), the absence of calcification ($P < 0.01$; Fig. 8), the presence of hem-

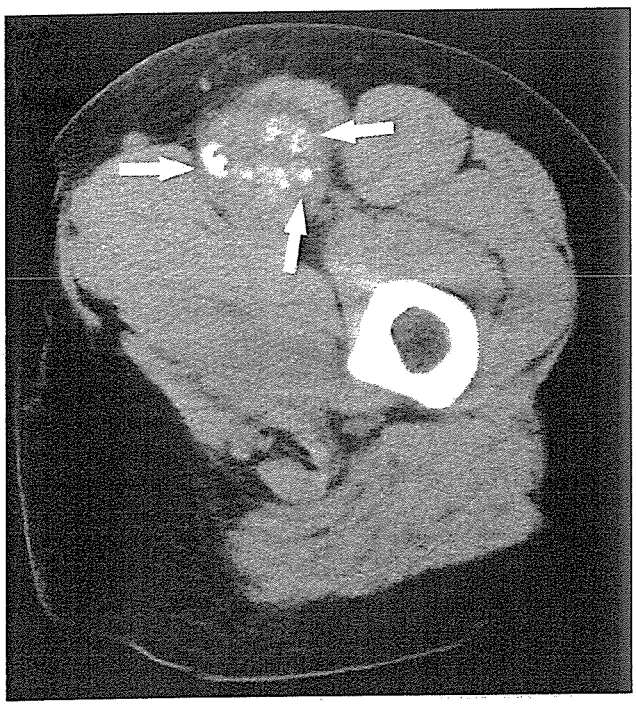

FIGURE 1. Unenhanced CT image obtained in a 14-year-old woman with synovial sarcoma (low-grade) of left groin. Image obtained at the level of inguinal region shows round or punctate calcifications (arrows) within the tumor.

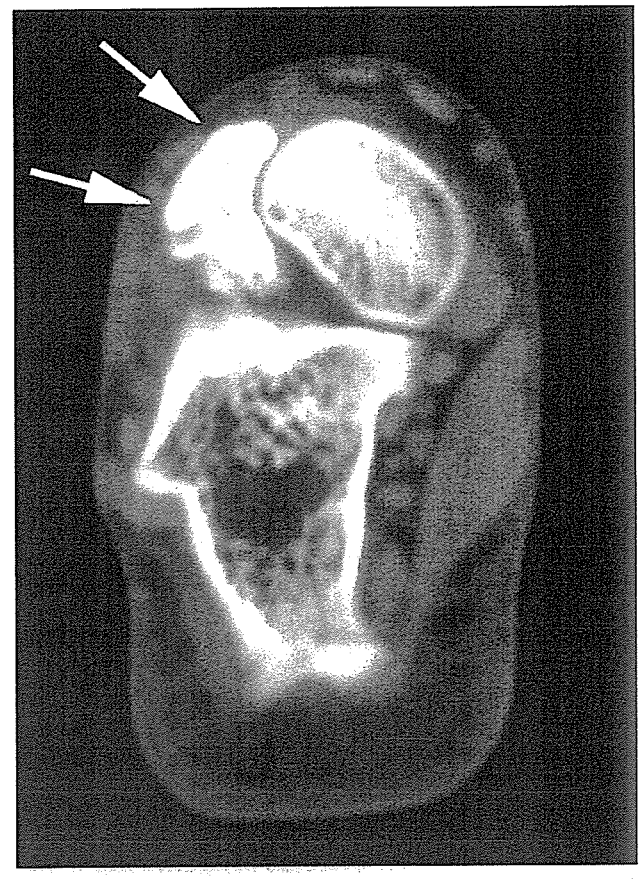

FIGURE 2. Unenhanced CT image obtained in a 14-year-old boy with synovial sarcoma (low-grade) of left foot. Image obtained at the level of talus head shows a dense calcification (arrows).

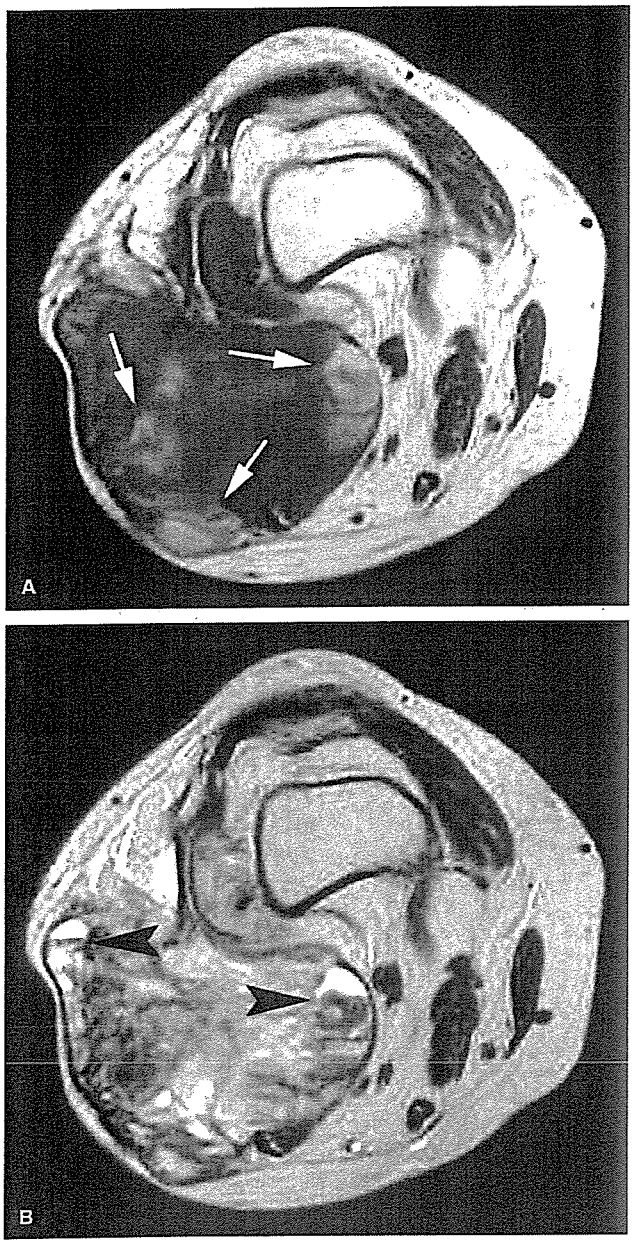

FIGURE 3. A 57-year-old woman with synovial sarcoma (high-grade) in left knee. A, Axial T1-weighted spin-echo (TR/TE: 720/50 milliseconds) MR image at the level of distal femur shows irregular soft tissue mass with multiple areas of high intensity signals (arrows). B, Axial T2-weighted fast spin-echo (3500/100) MR image shows fluid-fluid that suggests the presence of hemorrhage at the same location (arrowheads).

orrhage ($P < 0.05$; Fig. 9), and the presence of triple signal pattern ($P < 0.05$; Fig. 10) had a significant association with the DFS (Table 1). No significant impact on the DFS was found in patients' age, gender, operative margins, or with or without

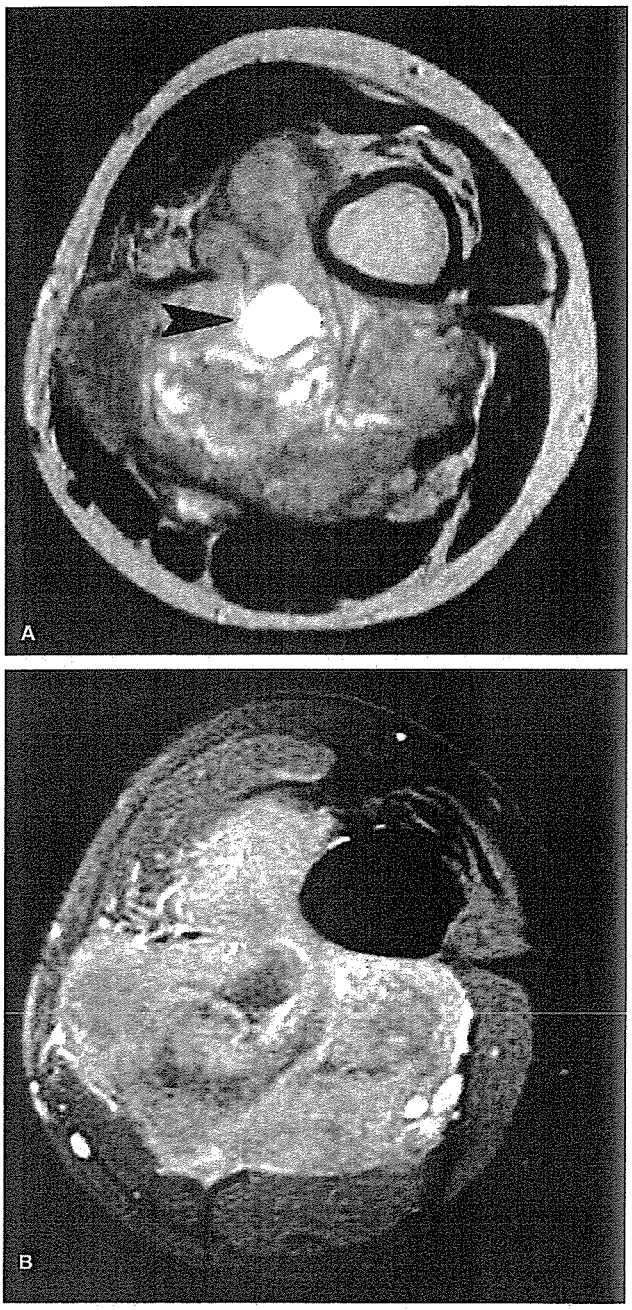

FIGURE 4. A 17-year-old man with synovial sarcoma (high-grade) in left thigh. A, Axial T2-weighted fast spin-echo (3500/100) MR image at the level of femur shows a large irregular mass of heterogeneous signal intensity. Also noted is central cystic degeneration (arrowhead). B, Fat-suppressed contrast-enhanced T1-weighted spin-echo (650/12) MR image demonstrates heterogeneous enhancement.

FIGURE 5. A 19-year-old woman with synovial sarcoma (high-grade) in right buttock. A, Coronal T2-weighted fast spin-echo (3500/100) MR image demonstrates triple signal pattern that includes high signal similar to that of fluid (arrows), intermediate signal intensity equal to or slightly hyperintense relative to fat (arrowheads), and low signal intensity closer to that of fibrous tissue (asterisk).

additional chemotherapy and radiotherapy. Imaging features including large tumor size ($P < 0.05$), the presence of internal septa ($P < 0.05$), and the presence of fluid-fluid levels ($P < 0.05$) were significantly associated with the MFS (Table 2). No statistically significant association was found between the RFS and the clinical or imaging features. Multiple logistic regression model showed that tumor size larger than 10 cm had a significant impact on the DFS with relative risk of 18.8 (95% confidence interval, 1.8–194.0, $P < 0.05$).

DISCUSSION

In the current study we have documented the prognostic significance of CT and MR imaging features in patients with synovial sarcoma of the soft tissues. Univariate analysis revealed that proximal distribution, hemorrhage, triple signal pattern, and calcification were significantly associated with overall survival. Synovial sarcomas of the soft tissues have been described as malignant mesenchymal tumors of uncertain origin with 5- and 10-year survival rates of 24% to 64% and 11% to 34%, respectively.[1,6] From a practical viewpoint, it seems useful to detect these imaging findings on CT or MR images in synovial sarcoma of the soft tissues to predict their behavior.

The radiologic appearance of smaller lesions can be well circumscribed and homogeneous, but is more frequently calcified than other soft tissue sarcomas. Calcification, present in approximately 30% of adult cases, may distinguish this lesion from other soft tissue sarcomas.[6,7] Twenty-eight percent of our cases had calcification within the tumor on CT scans which closely mirrored other published findings. Additionally, calcification in the stroma has been reported as a prognostic factor.[6] In our series, absence of calcification was a significant imaging finding favoring a diagnosis of high-grade tumor and was also significantly associated with poor prognosis. Therefore, to detect calcifications of synovial sarcoma of the soft tissues may be considered important and should be interpreted with CT scans.

High signal intensity on T1- and T2-weighted images corresponded to areas of hemorrhage identified pathologically as described in previous studies.[8,9] In our results, hemorrhage was found only in 12 patients with high-grade tumors and was a significant adverse prognostic factor. Triple signal pattern, one of the heterogeneous patterns on T2-weighted MR images, was also a significant adverse prognostic factor. Triple signal is considered to be not specific, but suggestive of the diagnosis given the most prevalent age.[8] Therefore, to detect this finding on T2-weighted MR images is relevant when evaluating patients with synovial sarcoma of the soft tissues. Fluid-fluid levels may occur whenever substances of differing densities are contained within a cystic or compartmentalized structure. The levels are depicted when imaging is performed in a gravity-dependent plane. Malignant tumors are often multiloculated, representing trapped fluid compartmentalized by thin bands of viable tumor. The presence of fluid-fluid levels in soft tissue tumors cannot be considered diagnostic of any particular tumor, including synovial sarcoma, hemangioma, or malignant fibrous histiocytoma.[18] A sign of fluid-fluid level was seen in 4 of our cases on T2-weighted MR images, which would suggest that this finding might be noteworthy but not specific in synovial sarcoma of the soft tissues. Concerning fluid-fluid levels, the MR appearance of mixed signal is often termed "bowl of fruit" because the various signal intensity areas resemble a collection of fruits, but this finding is not specific to synovial sarcoma and is also seen in malignant fibrous histiocytoma.[10] These MR findings of our cases, which included a heterogeneous, multilocular configuration with varying degrees of internal septa with or without fluid-fluid levels, agreed with those in previous descriptions of synovial sarcoma.[8]

Synovial sarcomas do not seem to enhance as markedly as tumors of vascular origin and are heterogeneous owing to the presence of degeneration including cyst, hemorrhage, or calcified regions of the tumor.[8–18] Tumors tend to have intermediate signal intensity on T1-weighted MR images. The T2-weighted signal intensity depends on the cellularity of the neoplasm; highly cellular types usually show intermediate signal intensity on T2-weighted images, and the stromal or less cellular variety have high T2-weighted signal intensity.[8–13] Fujimoto et al[11] reported a single case of synovial sarcoma of the chest wall in which the areas of low signal intensity on T1- and T2-weighted images corresponded to viable fibrous tissue of the tumor on pathologic correlation. The authors also de-

TABLE 1. Prognostic Factors for Disease-Free Survival (DFS) in Patients with Synovial Sarcoma of the Soft Tissues

Variable	5-Year DFS Rate (%)	n (%)	*P* Value
Age			0.39
<20 years	58	8 (26.7)	
≧20years	54	22 (73.3)	
Gender			0.59
Male	58	12 (40.0)	
Female	44	18 (60.0)	
Site			<0.05
Distal	89	13 (43.3)	
Proximal	23	17 (56.7)	
Size			<0.01
≦5 cm	86	12 (40.0)	
5–10 cm	0	10 (33.3)	
>10 cm	18	8 (26.7)	
Surgical margin			0.48
Adequate	47	16 (53.3)	
Inadequate	54	14 (46.7)	
Depth			0.61
Superficial	67	5 (16.7)	
Deep	43	25 (83.3)	
Stage			<0.01
IA	100	6 (20.0)	
IB	100	2 (6.7)	
IIB	100	8 (26.7)	
III	100	3 (10.0)	
IV	0	11 (36.7)	
Adjuvant therapy			0.14
None	88	8 (26.7)	
CTX and/or RTX	27	22 (73.3)	
Internal septa			0.09
Positive	80	10 (33.3)	
Negative	27	20 (66.7)	
Cyst			0.14
Positive	27	19 (63.3)	
Negative	78	11 (36.7)	
Calcification			<0.01
Positive	100	22 (73.3)	
Negative	0	8 (26.7)	
Hemorrhage			<0.05
Positive	0	16 (53.3)	
Negative	75	14 (46.7)	
Fluid-fluid levels			0.20
Positive	38	5 (16.7)	
Negative	50	25 (83.3)	
Triple signal pattern			<0.05
Positive	0	13 (43.3)	
Negative	76	17 (56.7)	
Enhancement			0.29
Homogeneous	75	5 (16.7)	
Heterogeneous	40	25 (83.3)	

Note: CTX, chemotherapy; RTX, radiotherapy.

TABLE 2. Prognostic Factors for Metastasis-Free Survival (MFS) in Patients with Synovial Sarcoma of the Soft Tissues

Variable	5-Year MFS Rate (%)	n (%)	*P* Value
Age			0.80
<20 years	60	8 (26.7)	
≧20 years	56	22 (73.3)	
Gender			0.93
Male	47	12 (40.0)	
Female	60	18 (60.0)	
Site			0.11
Distal	81	13 (43.3)	
Proximal	43	17 (56.7)	
Size			<0.05
≦5 cm	89	12 (40.0)	
5–10 cm	42	10 (33.3)	
>10 cm	31	8 (26.7)	
Surgical margin			0.25
Adequate	68	16 (53.3)	
Inadequate	46	14 (46.7)	
Depth			0.42
Superficial	67	5 (16.7)	
Deep	55	25 (83.3)	
Stage			<0.0001
IA	100	6 (20.0)	
IB	100	2 (6.7)	
IIB	100	8 (26.7)	
III	100	3 (10.0)	
IV	0	11 (36.7)	
Adjuvant therapy			0.30
None	75	8 (26.7)	
CTX and/or RTX	48	22 (73.3)	
Internal septa			<0.05
Positive	86	10 (33.3)	
Negative	45	20 (66.7)	
Cyst			0.24
Positive	68	19 (63.3)	
Negative	52	11 (36.7)	
Calcification			0.34
Positive	70	22 (73.3)	
Negative	52	8 (26.7)	
Hemorrhage			0.07
Positive	70	16 (53.3)	
Negative	44	14 (46.7)	
Fluid-fluid levels			<0.05
Positive	40	5 (16.7)	
Negative	62	25 (83.3)	
Triple signal pattern			0.11
Positive	41	13 (43.3)	
Negative	71	17 (56.7)	
Enhancement			0.64
Homogeneous	60	5 (16.7)	
Heterogeneous	58	25 (83.3)	

Note: CTX, chemotherapy; RTX, radiotherapy.

TABLE 3. Prognostic Factors for Recurrence-Free Survival (RFS) in Patients with Synovial Sarcoma of the Soft Tissues

Variable	5-Year RFS Rate (%)	n (%)	*P* Value
Age			0.27
<20 years	50	8 (26.7)	
≧20 years	72	22 (73.3)	
Gender			0.95
Male	67	12 (40.0)	
Female	63	18 (60.0)	
Site			0.08
Distal	89	13 (43.3)	
Proximal	53	17 (56.7)	
Size			0.74
≦5 cm	70	12 (40.0)	
5–10 cm	67	10 (33.3)	
>10 cm	57	8 (26.7)	
Surgical margin			0.26
Adequate	75	16 (53.3)	
Inadequate	57	14 (46.7)	
Depth			0.48
Superficial	50	5 (16.7)	
Deep	68	25 (83.3)	
Stage			0.53
IA	83	6 (20.0)	
IB	100	2 (6.7)	
IIB	80	8 (26.7)	
III	67	3 (10.0)	
IV	46	11 (36.7)	
Adjuvant therapy			0.13
None	88	8 (26.7)	
CTX and/or RTX	56	22 (73.3)	
Internal septa			0.89
Positive	63	10 (33.3)	
Negative	67	20 (66.7)	
Cyst			0.74
Positive	60	19 (63.3)	
Negative	69	11 (36.7)	
Calcification			0.87
Positive	65	22 (73.3)	
Negative	67	8 (26.7)	
Hemorrhage			0.46
Positive	57	16 (53.3)	
Negative	75	14 (46.7)	
Fluid-fluid levels			0.77
Positive	75	5 (16.7)	
Negative	64	25 (83.3)	
Triple signal pattern			0.08
Positive	50	13 (43.3)	
Negative	83	17 (56.7)	
Enhancement			0.36
Homogeneous	71	5 (16.7)	
Heterogeneous	40	25 (83.3)	

Note: CTX, chemotherapy; RTX, radiotherapy.

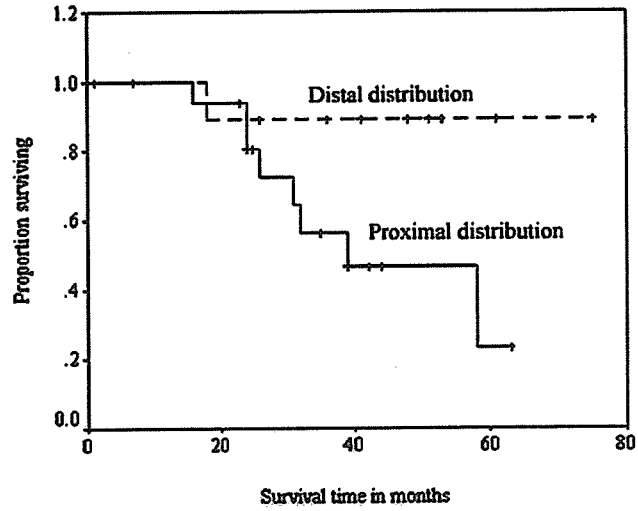

FIGURE 6. Influence of tumor site on the disease-free survival (DFS) in 30 patients with synovial sarcoma of the soft tissues ($P < 0.05$).

scribed that the areas of low signal intensity on T1-weighted images and high signal intensity on T2-weighted images also corresponded to viable portions.[10] Although tissue specimens revealed a biphasic nature within the tumors, no apparent correlation was found between the signal intensity on MR images and the fibrous content of the pathologic specimens.

The limitation of our study is that, given the limited number of patients and limited follow-up, multivariate analysis of the prognostic value of clinical and radiologic findings could not be performed. Whether CT and MR imaging parameters will add original information to the existing prognostic

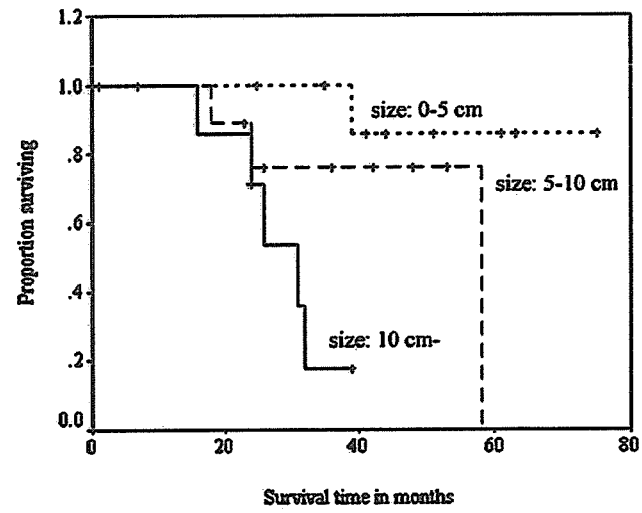

FIGURE 7. Influence of tumor size on the disease-free survival (DFS) in 30 patients with synovial sarcoma of the soft tissues ($P < 0.01$).

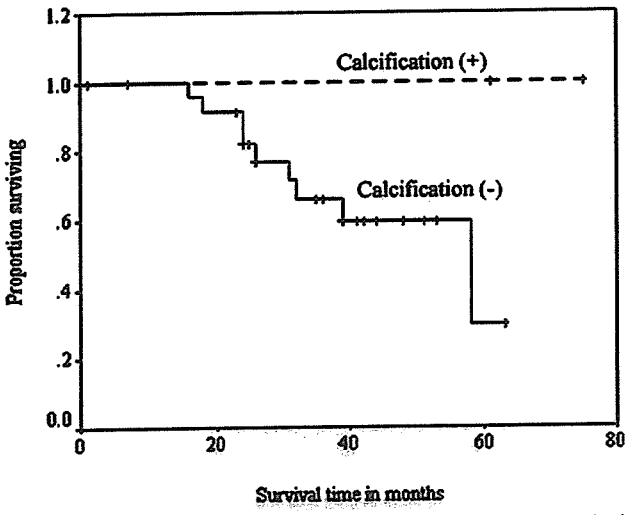

FIGURE 8. Influence of calcification on the disease-free survival (DFS) in 30 patients with synovial sarcoma of the soft tissues ($P < 0.01$).

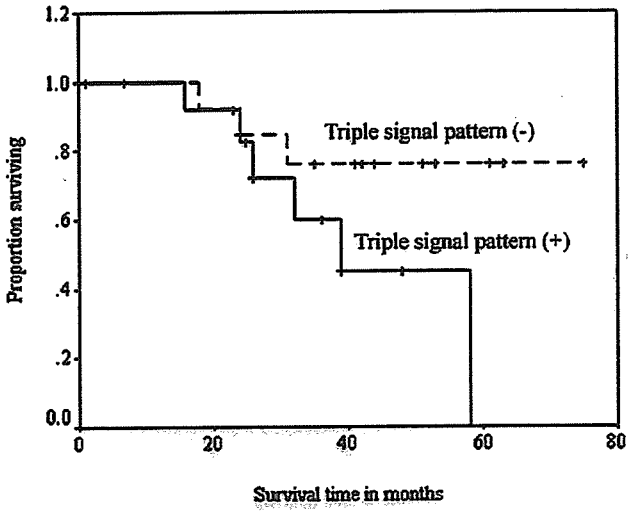

FIGURE 10. Influence of triple signal pattern on the disease-free survival (DFS) in 30 patients with synovial sarcoma of the soft tissues ($P < 0.05$).

variables requires further evaluation in an ongoing long-term study. Of several imaging findings, our results suggested that tumor size could help distinguish between low- and high-grade tumors. However, there was no association between tumor size and clinical outcome by univariate analysis. A retrospective study of 56 patients by Oda et al[22] suggested that large tumor size and extensive tumor necrosis are adverse prognostic factors. Blacksin et al[13] reported that one-third of synovial sarcomas approximately less than 5 cm in diameter had benign characteristics. Our relatively small sample size might affect the statistical analysis.

In conclusion, this study shows that CT and MR imaging findings can assist in distinguishing between low- and high-grade tumors in patients with synovial sarcoma of the soft tissues. Although these imaging findings cannot be considered specific for synovial sarcoma of the soft tissue, an awareness of the typical morphologic appearance may aid in predicting survival.

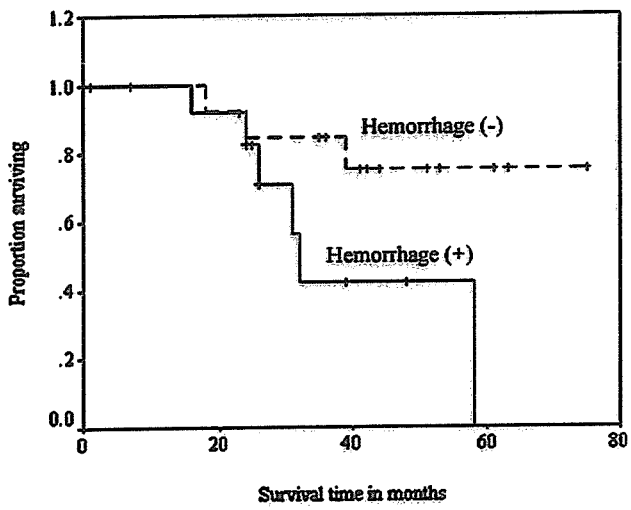

FIGURE 9. Influence of hemorrhage on the disease-free survival (DFS) in 30 patients with synovial sarcoma of the soft tissues ($P < 0.05$).

REFERENCES

1. Cadman NL, Soule EH, Kelly PJ. Synovial sarcoma. An analysis of 134 tumors. *Cancer*. 1965;18:613–627.
2. El-Nagger AK, Ayala AG, Abdul-Karim FW, et al. Synovial sarcoma. A DNA flow cytometric study. *Cancer*. 1990;65:2295–2300.
3. Enzinger FM, Weiss SW. *Soft Tissue Tumors*. 4th ed. St Louis, MO: Mosby–Year Book, 2001.
4. Evans H. Synovial sarcoma: a study of 23 biphasic and 17 probable monophasic examples. *Pathol Ann*. 1980;15:309–331.
5. Krall RA, Kostianovsky M, Patchefsky AS. Synovial sarcoma. A clinical, pathological, and ultrastructral study of 26 cases supporting the recognition of a monophasic variant. *Am J Surg Pathol*. 1981;5:137–151.
6. Cagle LA, Mirra JM, Storm FK, et al. Histologic features relating to prognosis in synovial sarcoma. *Cancer*. 1987;59:1810–1814.
7. Varela-Duran J, Enzinger FM. Calcifying synovial sarcoma. *Cancer*. 1982;50:345–352.
8. Fanney D, Castillo M, Lerner HH. Computed tomography of calcified synovial sarcoma of the hypopharynx. *J Compt Assist Tomogr*. 1988;12:687–689.
9. Jones BC, Sundaram M, Krandorf MJ. Synovial sarcoma: MR imaging findings in 34 patients. *AJR Am J Roentgenol*. 1993;161:827–830.
10. Morton MJ, Berquist TH, McLeod RA, et al. MR imaging of synovial sarcoma. *AJR Am J Roentgenol*. 1991;156:337–340.
11. Fujimoto K, Hashimoto S, Abe T, et al. Synovial sarcoma arising from the chest wall: MR imaging finding. *Radiation Med*. 1997;15:411–414.
12. Israels SJ, Chan HSL, Daneman A, et al. Synovial sarcoma in childhood. *AJR Am J Roentgenol*. 1984;142:803–806.

13. Blacksin MF, Siegel JR, Benevenia J, et al. Synovial sarcoma: frequency of nonaggressive MR characteristics. *J Compt Assist Tomogr*. 1997;21: 785–789.
14. Hirsch RJ, Yousem DM, Loevner LA, et al. Synovial sarcoma of the head and neck: MR findings. *AJR Am J Roentgenol*. 1997;169:1185–1188.
15. Mizutani H, Yanagi T, Suzuki H, et al. Synovial sarcoma in the prevertebral space of the neck: CT and MR findings. *Radiation Med*. 1997;15: 121–124.
16. Wu JW, Kahn SJ, Chew FS. Paraspinal synovial sarcoma. *AJR Am J Roentgenol*. 2000;174:410.
17. Kaakaji Y, Valle DE, McCarthy KE, et al. Musculoskeletal case of the day. Synovial sarcoma. *AJR Am J Roentgenol*. 1998;171:868–870.
18. Sigal R, Chancelier M, Luboinski B, et al. Synovial sarcoma of the head and neck: CT and MR findings. *AJNR Am J Neuroradiol*. 1992;13:1459–1462.
19. Hasegawa T, Yokoyama R, Lee YH, et al. Prognostic relevance of a histological grading system using MIB-1 for adult soft-tissue sarcoma. *Oncology*. 2000;58:66–74.
20. Hasegawa T, Yamamoto S, Yokoyama R, et al. Prognostic significance of grading and staging systems using MIB-1 score in adult patients with soft tissue sarcoma of the extremities and trunk. *Cancer*. 2002;95:843–851.
21. Hasegawa T, Yamamoto S, Nojima T, et al. Validity and reproducibility of histologic diagnosis and grading for adult soft-tissue sarcomas. *Hum Pathol*. 2002;33:111–115.
22. Oda Y, Hashimoto H, Tsuneyoshi M, et al. Survival of synovial sarcoma. A multivariate study of prognostic factors with special emphasis on the comparison between early death and long-term survival. *Am J Surg Pathol*. 1993;17:35–44.

AJR

American Journal of Roentgenology
Diagnostic Imaging and Related Sciences

Journal of the American Roentgen Ray Society Volume 182, No. 3, March 2004

Prognostic Significance of MRI Findings in Patients with Myxoid–Round Cell Liposarcoma

Ukihide Tateishi
Tadashi Hasegawa
Yasuo Beppu
Akira Kawai
Mitsuo Satake
Noriyuki Moriyama

Prognostic Significance of MRI Findings in Patients with Myxoid–Round Cell Liposarcoma

Ukihide Tateishi[1]
Tadashi Hasegawa[2]
Yasuo Beppu[3]
Akira Kawai[3]
Mitsuo Satake[1]
Noriyuki Moriyama[1]

OBJECTIVE. The aims of this study were to determine the prognostic significance of MRI findings in patients with myxoid–round cell liposarcomas and to clarify which MRI features best indicate tumors with adverse clinical behavior.

MATERIALS AND METHODS. The initial MRI studies of 36 pathologically confirmed myxoid–round cell liposarcomas were retrospectively reviewed, and observations from this review were correlated with the histopathologic features. MR images were evaluated by two radiologists with agreement by consensus, and both univariate and multivariate analyses were conducted to evaluate survival with a median clinical follow-up of 33 months (range, 9–276 months).

RESULTS. Statistically significant MRI findings that favored a diagnosis of intermediate- or high-grade tumor were large tumor size (> 10 cm), deeply situated tumor, tumor possessing irregular contours, absence of lobulation, absence of thin septa, presence of thick septa, absence of tumor capsule, high-intensity signal pattern, pronounced enhancement, and globular or nodular enhancement. Of these MRI findings, thin septa ($p < 0.05$), a tumor capsule ($p < 0.01$), and pronounced enhancement ($p < 0.01$) were associated significantly, according to univariate analysis, with overall survival. Multivariate analysis indicated that pronounced enhancement was associated significantly with overall survival ($p < 0.05$).

CONCLUSION. Contrast-enhanced MRI findings can indicate a good or adverse prognosis in patients with myxoid–round cell liposarcomas.

Liposarcomas are classified into well-differentiated, myxoid, round cell, and pleomorphic subtypes. Myxoid liposarcomas are the most common subtype of liposarcoma, occurring in the extremities of adults. They are considered low-grade sarcomas with a low risk of metastasis and are associated with prolonged survival [1–5]. On the other hand, round cell liposarcomas are considered high-grade sarcomas with a higher likelihood of metastasis and mortality due to disease [1–5]. Recent studies reveal that myxoid and round cell liposarcomas belong to a continuous histopathologic spectrum characterized by a chromosome translocation t(12;16)(q13;p11) resulting in the fusion transcript of the *TLS* and *CHOP* genes [6–9]. However, diagnosis and prognostic predictions can often be complicated by lesions that contain admixed morphologic components of myxoid and round cell subtypes.

The characteristic MRI features of myxoid–round cell liposarcomas are attributable to the predominantly myxoid matrix of the tumor. Tumors appear on T2-weighted MR images as encapsulated tumors with signals that are hyperintense compared with the surrounding structures [10–14]. On contrast-enhanced studies, they often show marked or heterogeneous enhancement with nonenhanced areas corresponding to myxoid material [13, 14]. As expected from the fact that the histopathologic spectrum from myxoid to round cell liposarcomas is continuous, these tumors show considerable diversity on imaging. Therefore, it is important to review the reliability of MRI features for characterizing myxoid–round cell liposarcomas. The objectives of this study were to determine the prognostic significance of MRI findings in patients with myxoid–round cell liposarcomas and to clarify which MRI features best indicate tumors with adverse clinical behavior.

Received February 3, 2003; accepted after revision July 11, 2003.

[1]Division of Diagnostic Radiology, National Cancer Center Hospital and Research Institute, Tsukiji, Chuo-Ku, Tokyo 104-0045, Japan. Address correspondence to U. Tateishi.

[2]Division of Pathology, National Cancer Center Hospital and Research Institute, Tsukiji, Chuo-Ku, Tokyo 104-0045, Japan.

[3]Division of Orthopedics, National Cancer Center Hospital and Research Institute, Tsukiji, Chuo-Ku, Tokyo 104-0045, Japan.

AJR 2004;182:725–731

0361–803X/04/1823–725

Materials and Methods

Patients

We reviewed materials from 36 patients with myxoid–round cell liposarcomas, all of whom who were registered in our pathology files. The clinical details, including follow-up information, were obtained by reviewing all the medical charts. None of the patients was lost to follow-up, which began on the date of primary surgery. The median duration of follow-up was 33 months and ranged from 9 to 276 months. The time to death due to any cause was recorded to determine the overall survival rate.

MRI Studies and Pathologic Correlations

MRI was performed using one of two 1.5-T systems (Horizon, General Electric Medical Systems, Milwaukee, WI; or Visart, Toshiba Medical Systems, Tokyo, Japan). Either the spin-echo or the fast spin-echo technique was used to obtain T1-weighted images (TR range/TE range, 460–720/12–27) in one or more planes (coronal or axial). T2-weighted images (TR range/TE_{eff} range, 3,500–6,000/96–112; echo-train length, 8–12) with flow compensation and presaturation superiorly and inferiorly were then obtained in one or more planes using a body coil. The images were obtained with a field of view of 30–40 cm, an image matrix of 128 × 256, and a slice thickness of 6–10 mm. Gadopentetate dimeglumine was administered IV, and T1-weighted images were obtained in one or more planes with (n = 20) or without (n = 16) fat suppression.

Two radiologists reviewed the MR images, and the findings were reported as a consensus opinion. The lesions were judged according to size, location, depth (superficial or deep), type of margin and contours, internal architecture, presence of a tumor capsule, signal characteristics on T1- and T2-weighted images, and homogeneity (homogeneous or heterogeneous). A superficial tumor (dermal or subcutaneous tumor) was located exclusively above the superficial fascia without invasion of the fascia, whereas a deep tumor was located either exclusively beneath the superficial fascia or superficial to the fascia with invasion of or through the fascia. The signal characteristics were described as isointense or hyperintense relative to the signal intensity of skeletal muscle. The extent (none and weak or pronounced), pattern (globular and nodular or diffuse), and homogeneity of gadolinium-based enhancement were also recorded. Globular and nodular enhancement corresponded to spotty enhancement (range, 3–10 mm) within the mass on contrast-enhanced MR images. Septal structures were categorized as thin (uniform linear structures ≤ 2 mm) or thick (focally thickened linear structures > 2 mm). Tumors containing areas with high-intensity characteristics on both T1- and T2-weighted MR images were considered positive for a high-intensity signal pattern.

Histologic slides of all the patients' tumors were reviewed for diagnosis by an expert pathologist. Immunohistochemical staining was performed in all cases to confirm the diagnosis or tumor type according to the classification system described by Enzinger and Weiss [1]. In this study, the histologic grade of a tumor was determined using a three-grade system established by Hasegawa et al. [15–17]. According to this system, myxoid–round cell liposarcomas are assigned a grade of 1, 2, or 3. Grade 1 tumors (n = 12, 33.3%) are considered low-grade tumors, grade 2 tumors (n = 14, 38.9%) are intermediate-grade tumors, and grade 3 tumors (n = 10, 27.8%) are high-grade tumors (n = 24, 66.7%). Excised specimens were available for review or for mapping correlation with images. Pathology reports were reviewed for descriptive comments characterizing the necrosis and myxoid–round cell tumor components of the lesions.

Statistical Analysis

Patients' demographics and imaging characteristics were compared using Wilcoxon's rank sum test for continuous variables and the chi-square test or Fisher's exact test for categorized variables. Univariate analysis was performed by comparing survival curves generated using the Kaplan-Meier method and carrying out log-rank tests. The relative risk of each variable subjected to multivariate analysis was estimated using a Cox proportional hazards model. All analyses were conducted using SPSS software version 11.0J (Statistical Package for the Social Sciences, Chicago, IL) for Windows (Microsoft, Redmond, WA). Differences and correlations at a p value of less than 0.05 were considered statistically significant.

Results

Twenty-one (58.3%) of the 36 patients were men and 15 were women (41.7%). The mean age at diagnosis was 47 years, and the patients ranged in age from 17 to 87 years. The tumors were located on the lower extremities in 31 patients (86.1%) and the trunk in five (13.9%). The mean tumor size was 9.6 cm, and 16 tumors (44.4%) were larger than 10 cm. Thirty-one tumors (86.1%) were situated deeply, and five (13.9%) were superficial. The surgical procedures consisted of wide excision, amputation, or disarticulation. Surgical margins were confirmed to be adequate at pathology in 28 patients (77.8%). Marginal or intralesional excision with inadequate margins were found in eight (22.2%). Additional treatment included chemotherapy in five patients (13.9%), radiotherapy in nine (25.0%), and both in seven (19.4%).

Metastases occurred in 11 (30.6%) of the 36 patients; the location of metastasis was the peritoneal cavity in five patients (13.9%); soft-tissue in five (13.9%); lung in three (8.3%); and bone, liver, retroperitoneum, and mediastinum in one (2.8%). Eight (38.0%) of the 21 patients who received additional treatment had metastasis subsequently. Twelve (33.3%) of the 36 patients developed local recurrences. Three patients (8.3%) with inadequate excision had local recurrence. Four patients (11.1%) with local recurrence underwent additional therapy.

Ten (27.8%) and 26 (72.2%) of 36 tumors had regular and irregular tumor contours, respectively (Figs. 1–4). Sixteen tumors (44.4%) showed lob-

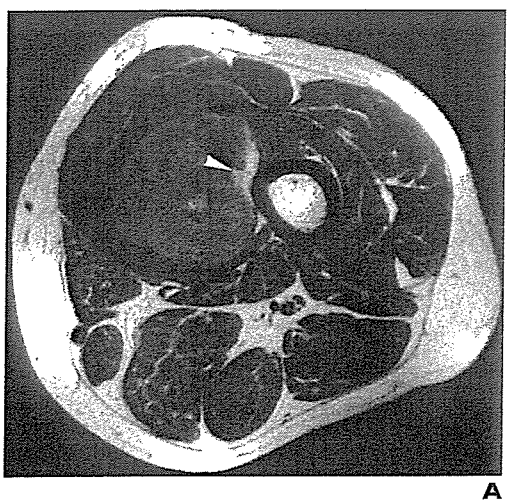

A

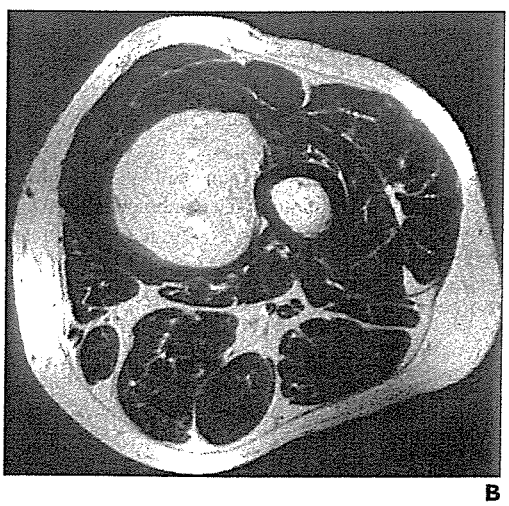

B

Fig. 1.—38-year-old woman with low-grade myxoid–round cell liposarcoma in left thigh.
A, T1-weighted spin-echo MR image (TR/TE, 720/20) shows tumor has regular contours with small amount of fat signal in periphery (*arrowhead*).
B, Contrast-enhanced T1-weighted spin-echo MR image (720/20) shows diffuse enhancement of tumor.